We are IntechOpen, the world's leading publisher of Open Access books Built by scientists, for scientists

4,800
Open access books available

122,000
International authors and editors

135M
Downloads

Our authors are among the

154
Countries delivered to

TOP 1%
most cited scientists

12.2%
Contributors from top 500 universities

CLARIVATE ANALYTICS BOOK CITATION INDEX INDEXED

WEB OF SCIENCE™

Selection of our books indexed in the Book Citation Index in Web of Science™ Core Collection (BKCI)

Interested in publishing with us?
Contact book.department@intechopen.com

Numbers displayed above are based on latest data collected.
For more information visit www.intechopen.com

1

Effects of Fuel Properties on Diffusion Combustion and Deposit Accumulation

Kazuhiro Hayashida[1] and Katsuhiko Haji[2]
[1]*Department of Mechanical Engineering, Kitami Institute of Technology*
[2]*Advanced Technology and Research Institute, Petroleum Energy Center (PEC)*
(Present affiliation: Research & Development Division
JX Nippon Oil & Energy Corporation)
Japan

1. Introduction

Petroleum is still the major source of energy in the world; petroleum-based fuels are used to various combustion devices, such as automotive engines, gas turbines and industrial furnaces. Combustion of petroleum-based fuels generates undesirable exhaust emissions (e.g. unburnt hydrocarbons, NOx, soot particles), and exhaust emissions from combustion devices cause serious problems to the environment and human health. Adjustment of the properties of the fuels is an effective way to improve the combustion characteristics so that minimize pollutant emissions. Basic knowledge of relationship between the fuel properties and practical combustion performances is necessary to make effective adjustments corresponding to the ongoing diversification of fuels, such as newly-introduced crude oil, sulfur-free fuel, and synthetic fuel (Iwama, 2005).

It is well known that combustion characteristic of liquid fossil fuels vary by fuel properties, such as distillation characteristics and hydrocarbon components (Kök & Pamir, 1995). Especially in the case of diffusion combustion, soot emission is strongly affected by fuel properties (Kidoguchi et al., 2000). Diffusion combustion is widely applied to various combustion devices, but the influence of fuel properties on diffusion combustion is not fully understood. Moreover, when combustion devices are used for a long time, deposits gradually accumulate on the parts of the device that are exposed to high temperatures, such as the fuel nozzle and the combustion chamber wall (Zerda, 1999). Accumulation characteristics of deposits are also strongly affected by changes in the properties of the fuel used. Since excessive deposit accumulation can cause malfunctions of combustion devices, such as decreased output and degradation of exhaust emissions, understanding of the relationship of fuel properties to deposit accumulation is important.

The effects of fuel properties on diffusion combustion and deposit accumulation are described in this article. Several types of kerosene fraction, which have different fuel properties, were used as the test fuels. A wick combustion burner was used to form a stable laminar diffusion flame of liquid fuel; the difference of diffusion combustion characteristics was investigated. Moreover, the effects of fuel properties on deposit accumulation were investigated through deposit accumulation on wick during wick combustion.

2. Experimental apparatus

2.1 Wick combustion burner

A wick flame was formed with a wick combustion burner, as shown in Fig. 1. The burner was equipped with a pool filled with fuel, and a wick was put in the pool. Fuel was supplied from a tank to the pool through a float chamber under the fuel tank. To form a steady flame, the fuel level within the pool was kept constant by the float. The fuel flow rate was derived from the weight loss of the burner, measured by an electronic balance. The pool was made of aluminium. The pool had an outer diameter of 20 mm, an inner diameter of 16 mm, and a depth of 6 mm. The wick, made of sintered bronze metal (39 % porosity), was placed in the centre of the pool. The wick was cylindrical (8 mm diameter, 18 mm length, 6 mm wall thickness) with a flat bottom (8 mm diameter, 2 mm thickness). The wick was put in the pool so that the bottom protruded 7 mm from the pool rim. The distance from the fuel surface to top of the wick was 10 mm.

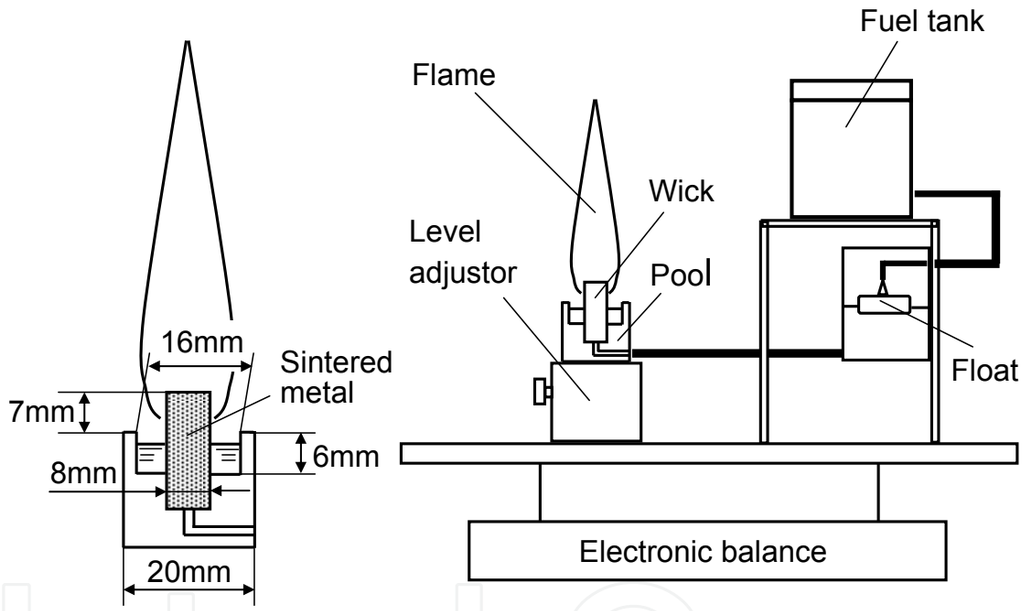

Fig. 1. Schematic of wick combustion burner

2.2 Laser diagnostic system

Laser diagnostic techniques are able to probe combustion products nonintrusively. Laser-induced fluorescence (LIF) and laser-induced incandescence (LII) are attractive techniques for combustion diagnostic and can be used to obtain information about PAHs (Hayashida, 2006) and soot (Shaddix, 1996), respectively. We measured the two-dimensional distribution of the PAHs-LIF in diffusion flames, and laser-induced incandescence (LII) was also used to visualize the soot distribution. Figure 2 shows schematic of the optical arrangement. The laser diagnostic system consisted of an Nd: YAG laser (Spectron Laser Systems, SL856G), a dye laser (Lumonics, HD-300B), and a doubling unit (Lumonics, HT-1000). The laser light was formed into a light sheet (0.5 mm×46 mm) by cylindrical lenses and was introduced into a target flame. Laser-induced emissions were detected by an ICCD camera (Andor

Technology, DH-534-18F-03), which was oriented perpendicular to the laser beam direction. The LIF and LII images were obtained by averaging 20 laser shots. For the PAHs-LIF measurement, the Nd: YAG laser was used to pump the dye laser (Rhodamine 590), producing a beam at 563 nm, and the doubling unit was used to double the dye laser output to produce 281.5 nm radiation. For the LII measurement, second harmonic generation (532 nm) of the Nd: YAG laser was used.

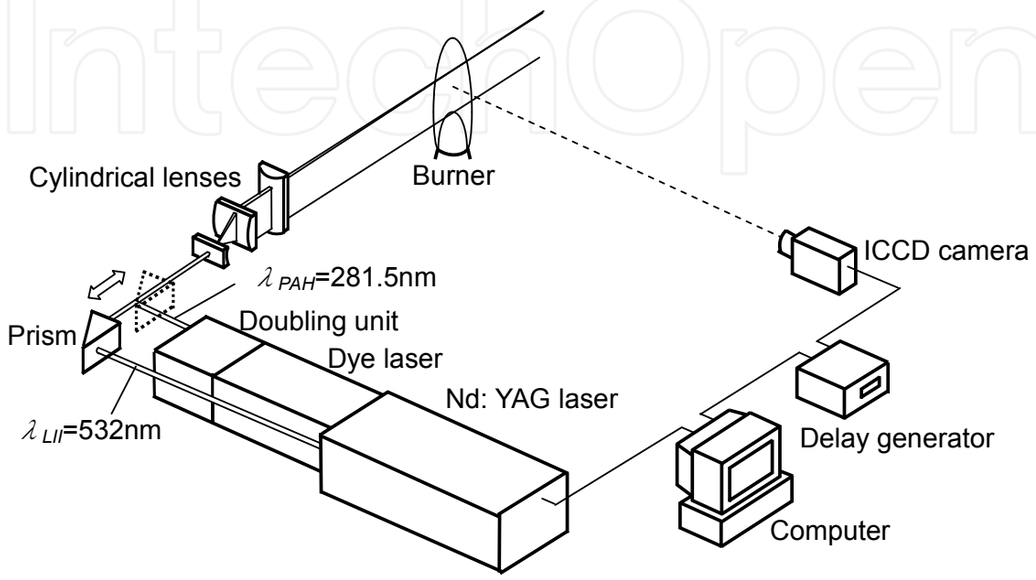

Fig. 2. Schematic of laser diagnostic system

3. Effects of fuel properties on diffusion combustion

3.1 Test fuels

Six types of fuel, with different distillation and compositional properties, were used. The physical properties of the test fuels are shown in Table 1. The calorific value of each fuel was same level, because the difference of net calorific value between test fuels was within 2.5%. Regarding fuel F, its smoke point (>50 mm) implies that the sooting tendency of fuel F was much smaller than that of the other fuels. Distillation characteristics indicate that fuel C was light, whereas fuel D was heavy in the test fuels. Fuel F was comparatively light, and fuel A, B and E had similar distillation characteristics. Influence of sulphur and nitrogen compounds on combustion was negligibly-small, because the contents of sulphur and nitrogen were extremely low.

Table 2 shows the results of the composition analyses of the test fuels. Although content of n-paraffin was not much difference between test fuels (28.6~34.4 vol%), there was considerable difference of i-paraffin content such as the fuel F (57.8 vol%) and fuel C (12.1 vol%). Content of naphthene hydrocarbons was low in fuel F (12.4 vol%) and comparatively low in fuel A (23.5 vol%). Aromatic hydrocarbons were much contained in fuel C (23.3 vol%), and were little contained in fuel E (9.9 vol%). Fuel F did not have any aromatics. Most of the aromatic components of the test fuels were one-ring aromatics; two-ring aromatics were very rare.

Fuel name		A	B	C	D	E	F
Density (15°C) [g/cm³]		0.7912	0.8007	0.8011	0.8000	0.7945	0.7547
Distillation characteristics	Initial boiling point [°C]	149.0	156.5	148.5	149.5	154.5	157.0
	5 vol% [°C]	163.5	169.5	160.5	165.5	168.5	165.5
	10 vol% [°C]	166.0	173.5	161.0	169.5	172.5	166.0
	20 vol% [°C]	173.0	179.5	165.5	178.0	179.5	169.5
	30 vol% [°C]	180.0	186.0	168.5	185.5	184.5	173.0
	40 vol% [°C]	187.0	193.0	172.0	194.0	191.0	177.5
	50 vol% [°C]	195.5	201.0	175.0	203.0	198.0	183.0
	60 vol% [°C]	204.5	210.5	179.0	213.0	204.5	190.5
	70 vol% [°C]	215.0	221.0	183.5	225.0	212.5	200.5
	80 vol% [°C]	227.5	233.5	189.5	237.0	222.5	214.5
	90 vol% [°C]	243.0	247.0	198.0	252.0	236.0	231.0
	95 vol% [°C]	253.0	257.5	205.5	262.0	247.0	240.0
	97 vol% [°C]	259.0	262.5	209.5	268.0	253.0	244.0
	End point [°C]	267.0	271.5	221.5	273.5	260.0	246.5
	Percent recovery [vol%]	98.5	98.5	98.5	98.5	98.5	98.5
	Percent residue [vol%]	1.0	1.0	1.0	1.0	1.0	1.0
	Percent loss [vol%]	0.5	0.5	0.5	0.5	0.5	0.5
Kinematic viscosity (30°C) [mm²/s]		1.361	1.475	1.096	1.501	1.455	1.322
Elemental analysis	Sulphur [mass ppm]	6	7	21	32	3	<1
	Nitrogen [mass ppm]	<1	<1	<1	<1	<1	<1
	Carbon [mass%]	86.0	86.1	86.3	86.0	85.7	84.5
	Hydrogen [mass%]	14.0	13.9	13.4	13.9	14.2	15.2
Net calorific value [J/g]		43380	43280	43000	43310	43440	44100
Smoke point [mm]		23.0	23	21.5	22.0	28.0	>50
Freezing point [°C]		-45.0	-45.0	-70.5	-42.5	-49.5	< -70.0
Flash point [°C]		43.5	47.0	40.5	45.5	46.5	46.0

Table 1. Physical properties of test fuels used in the diffusion combustion experiment

Component	Composition [vol%]					
	A	B	C	D	E	F
n-paraffins	34.4	32.0	28.6	30.4	29.5	29.8
i-paraffins	22.8	20.0	12.1	15.5	29.0	57.8
Mono-naphthenes	18.7	21.8	30.7	27.4	24.7	10.1
Di-naphthenes	3.9	5.2	4.1	6.6	5.4	2.3
Poly-naphthenes	0.9	1.2	1.2	1.2	1.4	0.0
Alkylbenzenes	12.7	10.8	19.9	10.6	6.1	0.0
Mono-naphtheno benzenes	5.3	6.5	1.6	6.1	3.3	0.0
Di-naphtheno benzenes	0.4	0.6	0.0	0.6	0.2	0.0
Poly-aromatics	1.0	1.9	1.8	1.5	0.3	0.0

Table 2. Composition of test fuels used in the diffusion combustion experiment

3.2 Flame temperature and flame luminosity

Figure 3 shows photographs of the test flames. Flame lengths of fuel C and F were longer than that of the other fuels because of relatively lower distillation temperature. Soot emissions from the flame tip were confirmed in every flame; amount of soot emission of fuel F was very low.

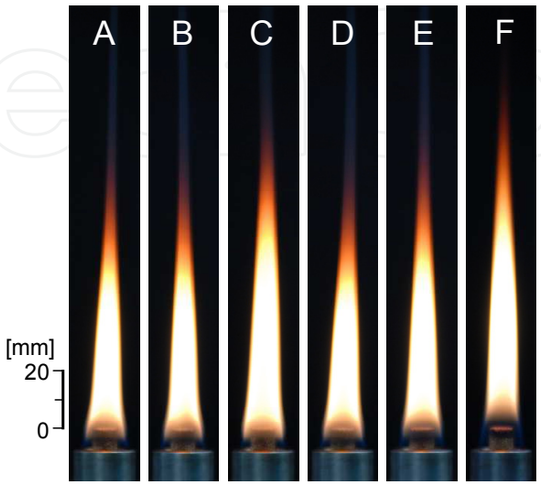

Fig. 3. Photographs of test flames

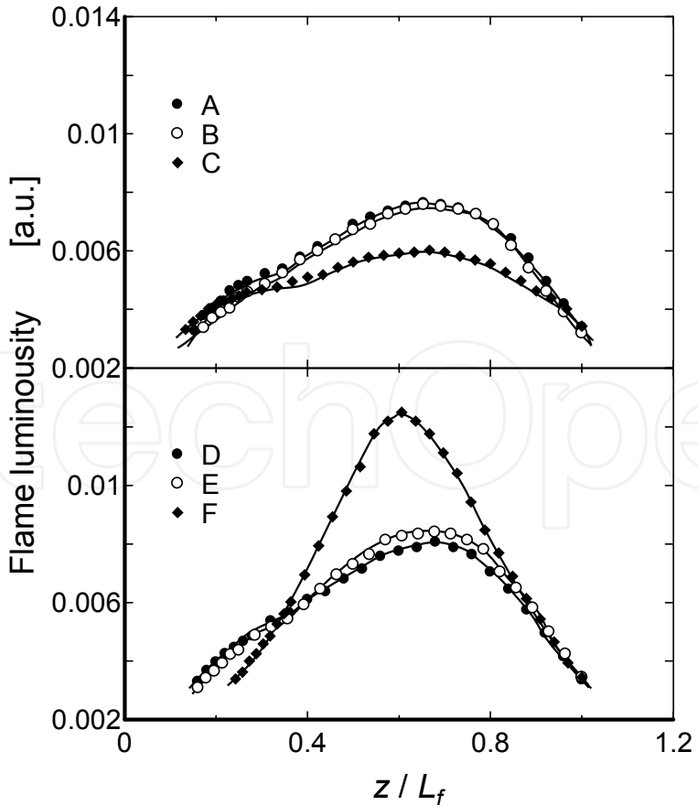

Fig. 4. Axial profiles of flame luminosities

Luminosity of the test flames at the centreline was measured by a CdS cell (wavelength sensitivity 400~800 nm, peak sensitivity 580 nm) through lens and pinhole. Obtained results were shown in Fig. 4. Note that measurement position was indicated as z/L_f. Here, z is distance from the wick and L_f is flame length from the wick; L_f is defined as flame luminosity disappearance position. Since electric resistance of CdS cell decreased with increasing the flame luminosity, the luminosity was expressed by inverse of CdS resistance. Flame luminosity of fuel F was particularly high, whereas luminosity of fuel C was lower than other fuels. The peak luminosity of fuel A, B, D and E was high in order of fuel E, D, A and B, and this order was corresponding to descending order of aromatic contents. According to the theory of black-body radiation, intensity of radiating body (i.e. soot particles) increases with temperature; thus the obtained luminosity would be reflected by flame temperature. Since soot is produced by the incomplete combustion of hydrocarbon fuel, it seems that the high luminosity of fuel F, which was lowest soot emission, was due to its high flame temperature resulting from the least incomplete combustion.

Figure 5 shows the temperature distributions of the test flames obtained by a two-color thermometer (Mitsui optronics, Thermera-seen). Here, two-color thermometer based on the two-color method (Zhao, 1998) measures the radiated energy of soot particles between two narrow wavelength bands, and calculates the ratio of the two energies, which is a function of the temperature. As for the black region in the figure, soot did not exist, or temperature and radiated energy of soot might be below the detection limit. Obtained result reveals that the temperature of flame F was particularly high.

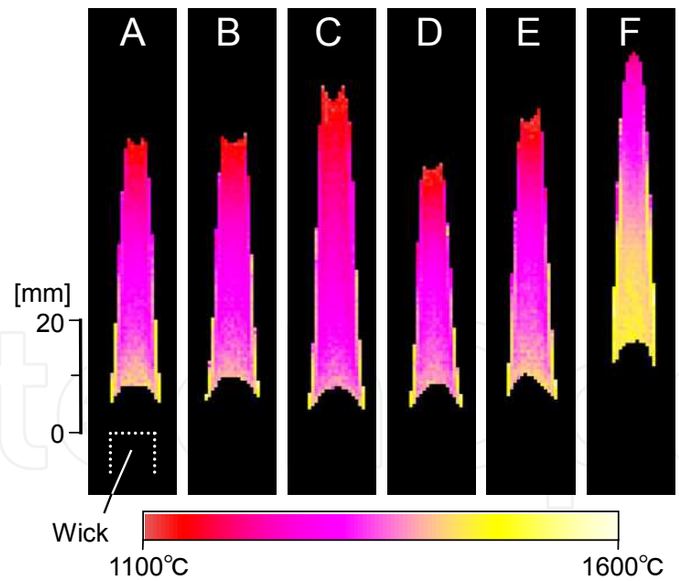

Fig. 5. Temperature distributions of the test flames

Figure 6 shows temperature profiles on centreline of the flame indicated in Fig. 5. The flame temperature of fuel F which did not contain aromatic compounds was the highest. Flame temperature was tendency to decrease in order of increasing aromatic components contained in the fuel, because soot generation within the flame might be increased with increasing the content of aromatics in the fuel.

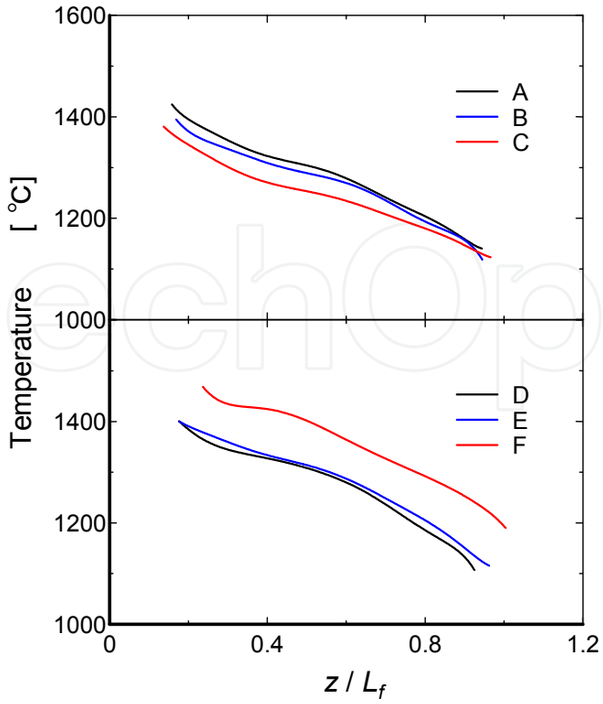

Fig. 6. Axial temperature profiles of the test flames

3.3 Concentration distributions of PAHs and soot

PAHs are considered to be precursors of soot particles formed in a flame, because it bridges the mass gap between fuel molecules and soot particles (Hepp, 1995). Formation and growth of PAHs arise from chemical reactions beginning with pyrolysis of fuel, and then inception of soot particles occurs by coagulation of grown PAHs. To estimate the effect of fuel properties on the soot emission and the soot generation characteristics, concentration distributions of soot and PAHs was investigated.

Figure 7 shows planar images of LII and PAHs-LIF obtained from the test flames. Since the concentrations of fuel F was significantly lower than the other fuels, another color scale was supplied in the figure. Except for fuel F, high concentration of LII at outer edge of the flame reveals that the soot was presence cylindrically in the flame. Regarding the fuel F, although the presence of soot was cylindrically in the lower part of the flame, upper part was not such distribution. LII distributions indicate that soot particles quickly formed in the case of fuel C and D. Since these fuels contain relatively much two-ring and poly-aromatics, soot particles might be promptly formed from those aromatics.

In each flame, PAHs-LIF was detected just after the wick, and the intensity decreases with increasing the distance from the wick. Regarding the fuel F, PAHs-LIF appeared comparatively strong between z=10~20 mm. A very low PAHs-LIF intensity of fuel F implies a very low PAHs concentration. It was confirmed that PAHs-LIF intensity became stronger with the aromatic contents increases.

Figure 8 shows the intensity profiles of PAHs-LIF and LII on the flame axis. Note that the PAHs-LIF intensity of fuel F was indicated as multiply the original data by 5. The peak of

the PAHs-LIF was located at just after the wick in any flames. Since fuel F did not contain any aromatics, the PAHs would be formed by pyrolysis of paraffin components and subsequent reactions within the wick. However, PAHs-LIF intensity of fuel F at just after the wick was much lower than that of the other fuels, thus the PAHs-LIF intensity detected at just after the wick of the other fuels might be derived mainly from the originally contained aromatics in the fuel. The PAHs-LIF intensity rapidly decreases with distance from the wick; this implies that the growth of PAHs occurred by condensation polymerization of PAHs and thereby the number of PAHs molecules decreases.

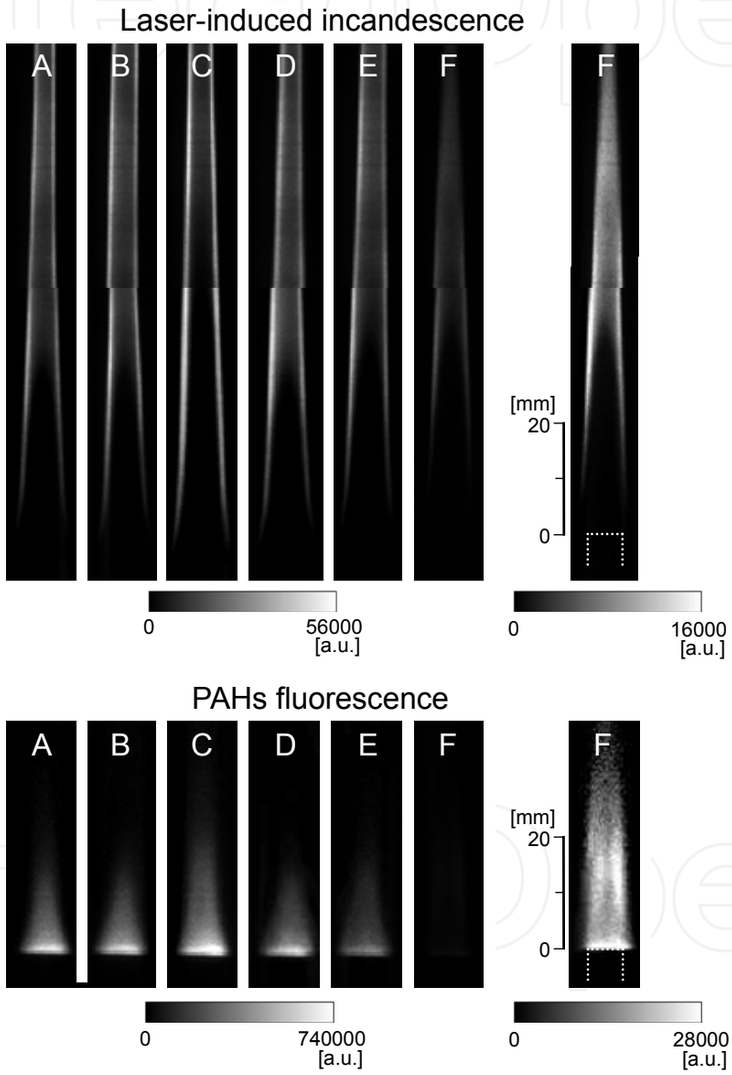

Fig. 7. Planar images of PAHs-LIF and LII

In the case of fuel F, increase of PAHs-LIF from z/L_f =0.15 suggested that the PAHs were newly formed within the flame. The same occurred within the other flames, but impact on the profile was small due to the relatively large LIF intensity of the originally contained PAHs. The disappearance location of the PAHs-LIF coincides with the location where the LII intensity rapidly increases. This figure clearly shows that the soot was formed via PAHs.

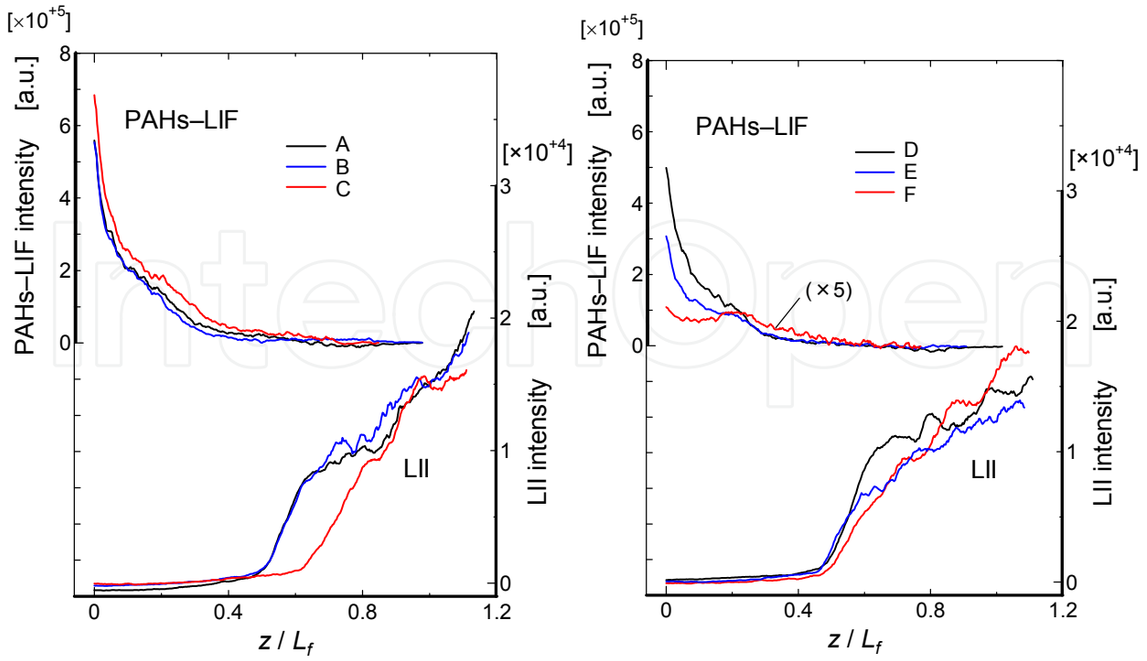

Fig. 8. Axial intensity profiles of PAHs-LIF and LII

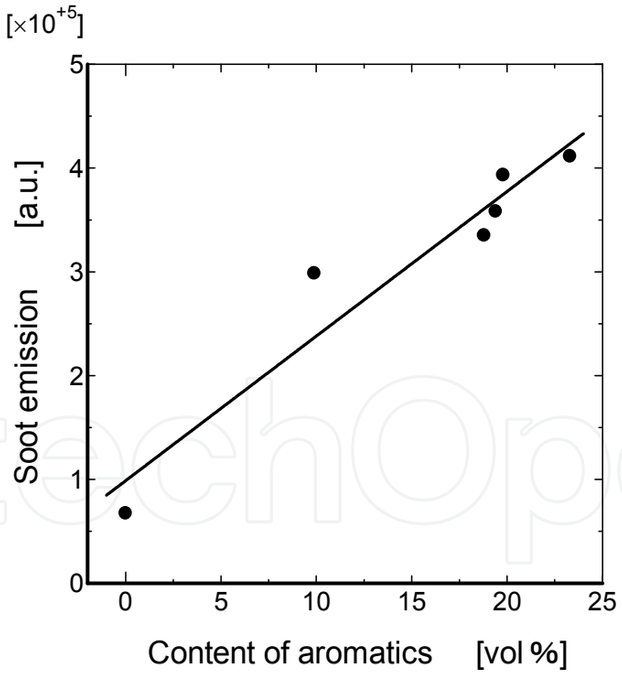

Fig. 9. Relationship between soot emission and content of aromatics

Figure 9 shows the relationship between soot emission from the test flames and content of aromatics in the test fuels. Soot emission was derived from total LII intensity at z=65mm, where combustion reaction seemed to be finished. Soot emission linearly increased with increasing content of aromatics.

4. Effects of fuel properties on deposit accumulation

4.1 Test fuels

Five types of kerosene fraction, with different distillation and compositional properties, were used. The physical properties of the test fuels are shown in Table 3. Regarding fuel K, the end point (246.5 °C) and density (0.7547 g/cm^3) were lower than those of the other fuels.

Test item		Test method	G	H	I	J	K
Density (15°C)[g/cm^3]		JIS K2249	0.7910	0.7895	0.7884	0.7980	0.7547
Distillation characteristics	Initial boiling point [°C]	JIS K2254	153.5	147.0	146.5	145.5	156.0
	5 vol% [°C]		166.0	161.0	161.5	158.0	164.5
	10 vol% [°C]		167.5	165.5	165.0	160.5	165.5
	20 vol% [°C]		174.5	172.5	171.5	167.0	168.5
	30 vol% [°C]		181.0	179.5	178.0	174.0	172.5
	40 vol% [°C]		187.5	187.0	184.5	182.0	177.5
	50 vol% [°C]		194.5	194.5	192.0	191.5	182.5
	60 vol% [°C]		202.5	204.0	201.0	201.5	190.5
	70 vol% [°C]		212.0	214.0	210.5	211.5	201.0
	80 vol% [°C]		223.0	227.0	225.5	223.0	215.0
	90 vol% [°C]		236.0	244.5	239.0	238.5	232.5
	95 vol% [°C]		246.0	259.5	254.0	249.0	242.0
	97 vol% [°C]		252.0	270.5	264.0	256.0	246.5
	End point [°C]		256.0	276.5	270.0	259.5	246.5
	Percent recovery [vol%]		98.5	98.5	98.5	98.5	98.5
	Percent residue [vol%]		1.0	1.0	1.0	1.0	1.0
	Percent loss [vol%]		0.5	0.5	0.5	0.5	0.5
Kinematic viscosity (30°C) [mm^2/s]		JIS K2283	1.347	1.365	1.335	1.373	1.334
Net calorific value [J/g]		JIS K2279	43380	43430	43440	43390	44100
Smoke point [mm]		JIS K2537	23.0	24.0	24.0	26.0	>50
Freezing point [°C]		JIS K2276	-48.5	-45.5	-49.0	-68.0	-66.0
Flash point [°C]		JIS K2265	45.0	43.5	44.0	39.5	46.0
Elemental analysis	Sulphur [mass ppm]	JIS K2541	8	4	2	<1	<1
	Nitrogen [mass ppm]	JIS K2609	<1	<1	<1	<1	<1
	Carbon [mass%]	JPI Method	85.8	85.9	85.6	85.8	84.6
	Hydrogen [mass%]	JPI Method	14.0	14.1	14.1	14.2	15.4
CH ratio		—	0.51437	0.51132	0.50953	0.50713	0.46107

Table 3. Physical properties of test fuels used in the deposit accumulation experiment

Table 4 shows the results of the composition analyses of the test fuels. The results confirmed that fuel K consisted only of saturated hydrocarbons (i.e., paraffins and naphthenes). In contrast, other fuels contained between 7.6~19.5 vol% aromatic hydrocarbons. Most of the aromatic components of the fuels were one-ring aromatics; two-ring aromatics were very rare. In addition, the following low-stability components are also shown in Table 4: naphtheno benzenes, olefin hydrocarbons (bromine number), dienes (diene value), and organic peroxides (peroxide number). Naphtheno benzenes, compounds that consist of naphthene and aromatic rings, were contained in higher concentrations in fuel G (5.4 vol%); these molecules were not contained in fuel K. The bromine number was largest in fuel J (28.8 $mgBr_2/100g$) and lowest in fuel K (4.4 $mgBr_2/100g$). The diene values of fuels J and K indicated 0.05 $gI_2/100g$ and 0.01 $gI_2/100g$, respectively; dienes were not detected in other fuels. The peroxide numbers demonstrate that none of the test fuels contained organic peroxides.

Component	G	H	I	J	K
Aromatic HC [vol%]	19.5	17.2	16.9	7.6	0.0
Unsaturated HC [vol%]	0.1	0.0	0.0	0.0	0.0
Saturated HC [vol%]	80.4	82.8	83.1	92.4	100.0
1-aromatics [vol%]	19.1	17.0	16.7	7.5	0.0
2-aromatics [vol%]	0.4	0.2	0.2	0.1	0.0
3^+-aromatics [vol%]	0.0	0.0	0.0	0.0	0.0
1-naphtheno benzenes [vol%]	5.0	4.8	4.2	2.5	0.0
2-naphtheno benzenes [vol%]	0.4	0.5	0.3	0.0	0.0
3^+-naphtheno benzenes [vol%]	0.0	0.0	0.0	0.0	0.0
Bromine number [$mgBr_2/100g$]	9.4	9.0	10.1	28.8	4.4
Diene value [$gI_2/100g$]	0.00	0.00	0.00	0.05	0.01
Peroxide number [mg/kg]	0.0	0.0	0.0	0.0	0.0

Table 4. Composition of test fuels used in the deposit accumulation experiment

4.2 Relationship between fuel properties and deposit accumulation

Tar-like deposits, formed by the thermal decomposition and polycondensation of the fuel, adhered to and accumulated on the upper part of the wick during combustion. To investigate the effects of fuel properties on tar-like deposit accumulation, tar-like deposits were accumulated on the wick by prolonged combustion. The deposit mass was obtained by subtracting the mass of unused wick from the mass of the wick that had accumulated deposits. In this process, if unburnt fuel remained in the wick with deposits, an accurate deposit mass could not be obtained. To eliminate remaining fuel, the wick was pulled up from the pool with a flame, and combustion was continued until all fuel was used. Obtained deposit was visually confirmed as tar-like deposit, but soot particle might have slightly adhered on the wick.

Figure 10 shows temporal change of deposit mass. In this experiment, one wick was sequentially used in the measurement of one test fuel. As seen in the figure, the deposit growth rate decreased after a certain period of time except fuel K. This result implies that the accumulation of deposits proceeded in two stages. Deposits were first rapidly accumulated in voids of the wick, which gradually saturate over time; we called this period the "internal accumulation mode". Once the voids became saturated with deposits, deposits subsequently accumulated on the outer surface of the wick; we called this phase the "surface growth mode". Although the deposit growth rate in the internal accumulation mode varied somewhat due to individual differences of the wick, the growth rate of the surface growth mode had reproducibility. Regarding fuel K, the deposit accumulation would not have attained to the surface growth mode owing to its extremely low deposit growth rate.

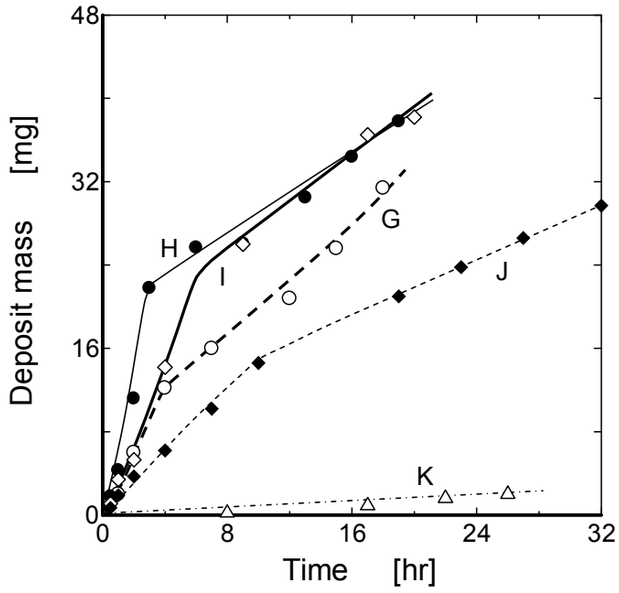

Fig. 10. Temporal change of deposit mass

As the deposit growth rate in the internal accumulation mode was influenced by individual differences of the wick, the relationship between deposit mass and fuel consumption was investigated in the surface growth mode. The results are shown in Fig. 11. Note that the results reported here for fuel K are not for the surface growth mode. Straight lines in the figure were obtained by the least-squares method, and the slopes correspond to the deposit accumulation ratio (the percentage of conversion from fuel to deposit). Deposit accumulation ratios are also indicated in the figure.

Obtained results indicate that the deposit mass of each fuel increased proportionally with increasing fuel consumption. Fuel G displayed the highest deposit accumulation ratio (0.00749 %), followed by fuel H (0.00580 %) and I (0.00574 %). Fuel K (0.00064 %) exhibited an extremely small accumulation ratio. Compared with the fuel compositions shown in Table 4, fuel G, with its high deposit accumulation ratio, was found to contain higher levels of aromatics and naphtheno benzenes; conversely, fuel K, with its low deposit accumulation ratio, contained no aromatics or naphtheno benzenes. Note that there was no correlation between the bromine number, diene value, and accumulation ratio. The extremely low

accumulation ratio of fuel K might be caused by several factors: (1) the amount of low-stability components in fuel K was very low, (2) pyrolysis of saturated hydrocarbons was hard to occur within the range of the internal temperature of the wick, and (3) deposits formation from the pyrolysis products of saturated hydrocarbons took relatively long time.

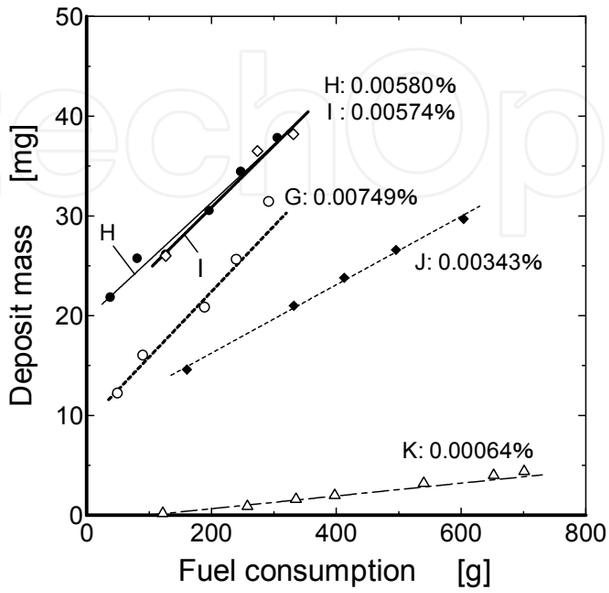

Fig. 11. Relationship between fuel consumption and deposit mass

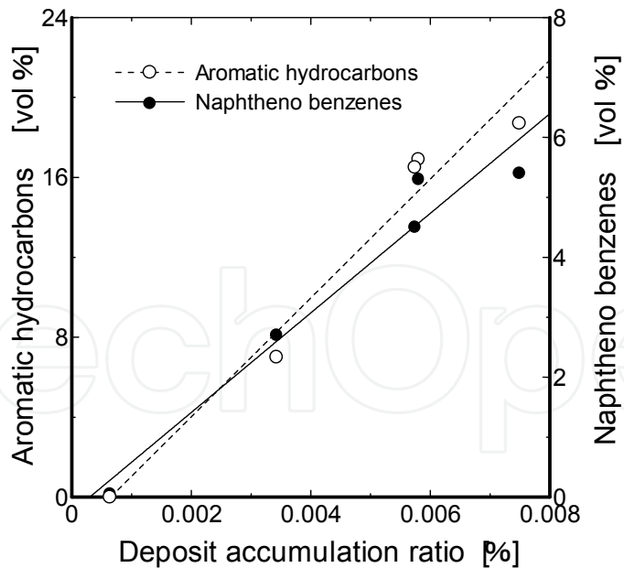

Fig. 12. Relationship between aromatic hydrocarbons, naphtheno benzenes and deposit accumulation ratio

The relationship between aromatic hydrocarbons, naphtheno benzenes and the deposit accumulation ratio is presented in Fig. 12. The deposit accumulation ratio was strongly associated with the content of aromatics and naphtheno benzenes. As naphtheno benzenes are

one of the aromatics, more naphtheno benzenes may be contained in the aromatic-rich fuel. It is well known that naphtheno benzenes are more susceptible to thermal decomposition at lower temperatures than other hydrocarbons; thus, pyrolysis and polycondensation of naphtheno benzenes would be performed within the wick. Finally, naphtheno benzenes were transformed into tar-like deposits. Conversely, because the pyrolysis of aromatics was difficult to perform due to their high thermal stability, initial aromatics contained in the fuel transformed into heavy molecules and tar-like deposit without pyrolysis. Note that the sooting tendency became stronger with increasing aromatic content in the fuel; soot adherence to the wick possibly affected the results shown in Fig. 12. Although the deposits did not necessarily originate from aromatics and naphtheno benzenes, the deposit accumulation ratio of fuel K was extremely low and no correlation was found between the bromine number, diene value, and deposit accumulation ratio. These results suggested that most of the deposits originated from the naphtheno benzenes and/or aromatic hydrocarbons.

4.3 Deposit analysis

Deposits that accumulated on the wick were extracted by diethyl ether and chloroform solutions and dried after evaporation of the solutions. The collected deposits were then analyzed with a simultaneous thermogravimetry/differential thermal analysis (TG-DTA) instrument (TA Instruments, SDT2960). Analysis was performed by the following steps:

1. The sample was held at room temperature for 5 minutes and then heated to 250 °C. (atmosphere: N_2, flow rate: 100 mL/min)
2. The sample was held at 250 °C for 10 minutes and then heated to 550 °C. (atmosphere: N_2, flow rate: 100 mL/min)
3. The sample was held at 550 °C for 20 minutes. (atmosphere: air, flow rate: 100 mL/min)

[heating rate; 50°C/min]

Table 5 shows the mass loss of the deposits in each step. Considering the boiling point of hydrocarbons, the mass loss of each step corresponds to (1) the kerosene fraction, (2) the heavy kerosene component and light polycondensation products of low molecular weight, and (3) the heavy polycondensation product. The residue was considered to be a carbonized deposit and soot particles.

Mass loss	G	H	I	J	K
Room temp.~250°C (N_2) [wt%]	15.0	12.5	12.5	15.1	14.2
250~550°C (N_2) [wt%]	22.2	23.2	18.0	21.4	26.4
550°C (air) [wt%]	49.5	51.1	61.4	62.8	60.0
Residue [wt%]	13.4	13.2	8.1	0.8	0.0

Table 5. Results of TG-DTA analysis

The results of TG-DTA analysis suggested that most of the deposit components were heavy polycondensation products formed by thermal decomposition and polycondensation of the fuel within the wick. Residues of fuel G, H and I, which contained higher amounts of aromatics and naphtheno benzenes, were higher than that of the other two fuels; this result

is probably due to an increase in the carbonized deposit formed at the wick surface and/or soot adhesion on wick. Additionally, some sulphur compounds might be contained in the residue because these fuels contain sulphur, as indicated in Table 3. In contrast, the deposits of fuel K contained no residue, and the mass loss in the range of 250~550 °C was relatively high. This fact demonstrates the very low deposit growth rate of fuel K, as described previously. The deposits of fuel J, with its very high bromine number and diene value, displayed a relatively large mass loss of the heavy polycondensation product; this observation may be due to the contribution of a tar-like deposit that originated from olefins and dienes (Zanier, 1998).

5. Conclusions

In this chapter, effects of fuel properties on diffusion combustion and deposit accumulation were studied experimentally. Obtained results could contribute to a design of fuel properties for reduction of the pollutant emissions from diffusion combustion of fossil fuels, and for suppression of the deposit accumulation within a combustion device.

5.1 Effects of fuel properties on diffusion combustion

Laminar diffusion flames of the test fuels were formed by using the wick combustion burner. Flame temperature and flame luminosity of each flame were measured. Furthermore, to investigate the effect on soot formation of fuel properties, concentration distributions of PAHs and soot were measured by LIF and LII. The main results are summarized as follows:

1. The peak luminosity of flame was high in order of decreasing aromatic components contained in the fuel.
2. Flame temperature tended to decrease with increasing aromatic components contained in the fuel.
3. In each flame, the PAHs-LIF intensity rapidly decreases with distance from the wick. The disappearance location of the PAHs-LIF coincides with the location where the LII intensity rapidly increases.
4. Soot emission increased with increasing content of aromatic hydrocarbons in the fuel.

5.2 Effects of fuel properties on deposit accumulation

Deposit accumulation processes were investigated by using the wick combustion burner. Deposit accumulation rate was estimated from the mass of deposit which accumulated on wick and the fuel consumption, and components of the deposit were estimated from the TG-DTA analysis. The main results are summarized as follows:

1. Except for fuel K, deposit accumulation per unit time (deposit growth rate) decreased after a certain time after ignition.
2. The conversion percentage from fuel to deposit (deposit accumulation ratio) increased with greater contents of aromatics and naphtheno benzenes in the fuels.
3. The primary components of deposits were heavy polycondensation products (50~60 wt%). Heavy kerosene components, light polycondensation products (about 20 wt%), and kerosene fractions (about 15 wt%) were also identified in the deposits.

6. Acknowledgement

This work was a cooperative research project with the Japan Petroleum Energy Center. We thank Prof. M. Arai and Prof. K. Amagai of Gunma University for helpful suggestions.

7. References

Hayashida, K., Amagai, K., Satoh, K. & Arai, M. (2006). Experimental Analysis of Soot Formation in Sooting Diffusion Flame by Laser-Induced Emissions. *Journal of Engineering for Gas Turbines and Power, Transactions of the ASME*, Vol.128, No.2, pp.241-246, ISSN 0742-4795

Hepp, H., Siegmann, K. & Sattler, K. (1995). New Aspects of Growth Mechanisms for Polycyclic Aromatic Hydrocarbons in Diffusion Flames. *Chemical Physics Letters*, Vol.233, No.1-2, pp.16-22, ISSN 0009-2614

Iwama, K. (2005). The Diversification of Energy Source in the New Era. *Journal of the Japanese Association for Petroleum Technology*, Vol.70, No.2, pp.125-131, ISSN 0370-9868

Kidoguchi, Y., Yang, C. & Miwa, K. (2000). Effects of Fuel Properties on Combustion and Emission Characteristics of a Direct-Injection Diesel Engine. *SAE paper 2000-01-1851*

Kök, M.V. & Pamir, M.R. (1995). Pyrolysis and Combustion Studies of Fossil Fuels by Thermal Analysis Methods. *Journal of Analytical and Applied Pyrolysis*, Vol.35, No.2, pp.145-156, ISSN 0165-2370

Shaddix, C.R. & Smyth, K.C. (1996). Laser-Induced Incandescence Measurements of Soot Production in Steady and Flickering Methane, Propane, and Ethylene Diffusion Flames. *Combustion and Flame*, Vol.107, No.4, pp.418-452, ISSN 0010-2180

Zanier, A. (1998). Thermal-Oxidation Stability of Motor Gasolines by Pressure d.s.c.. *Fuel*, Vol.77, No.8, pp.865-870, ISSN 0016-2361

Zerda, T.W., Yuan, X., Moore, S.M. & Leon y Leon, C.A. (1999). Surface Area, Pore Size Distribution and Microstructure of Combustion Engine Deposits. *Carbon*, Vol.37, No.12, pp.1999-2009, ISSN 0008-6223

Zhao, H. & Ladommatos, N. (1998). Optical Diagnostics for Soot and Temperature Measurement in Diesel Engines. *Progress in Energy and Combustion Science*, Vol.24, No.3, pp.221-255, ISSN 0360-1285

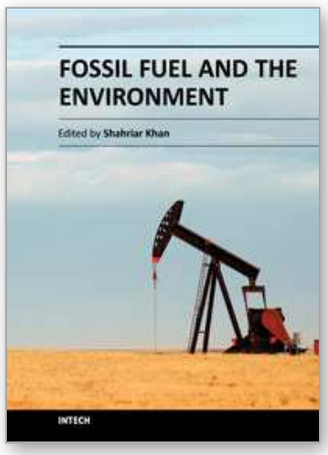

Fossil Fuel and the Environment

Edited by Dr. Shahriar Khan

ISBN 978-953-51-0277-9
Hard cover, 304 pages
Publisher InTech
Published online 14, March, 2012
Published in print edition March, 2012

The world today is at crossroads in terms of energy, as fossil fuel continues to shape global geopolitics. Alternative energy has become rapidly feasible, with thousands of wind-turbines emerging in the landscapes of the US and Europe. Solar energy and bio-fuels have found similarly wide applications. This book is a compilation of 13 chapters. The topics move mostly seamlessly from fuel combustion and coexistencewith renewable energy, to the environment, and finally to the economics of energy, and food security. The research and vision defines much of the range of our scientific knowledge on the subject and is a driving force for the future. Whether feasible or futuristic, this book is a great read for researchers, practitioners, or just about anyone with an enquiring mind on this subject.

How to reference

In order to correctly reference this scholarly work, feel free to copy and paste the following:

Kazuhiro Hayashida and Katsuhiko Haji (2012). Effects of Fuel Properties on Diffusion Combustion and Deposit Accumulation, Fossil Fuel and the Environment, Dr. Shahriar Khan (Ed.), ISBN: 978-953-51-0277-9, InTech, Available from: http://www.intechopen.com/books/fossil-fuel-and-the-environment/effects-of-fuel-properties-on-diffusion-combustion-and-deposit-accumulation

INTECH
open science | open minds

InTech Europe
University Campus STeP Ri
Slavka Krautzeka 83/A
51000 Rijeka, Croatia
Phone: +385 (51) 770 447
Fax: +385 (51) 686 166
www.intechopen.com

InTech China
Unit 405, Office Block, Hotel Equatorial Shanghai
No.65, Yan An Road (West), Shanghai, 200040, China
中国上海市延安西路65号上海国际贵都大饭店办公楼405单元
Phone: +86-21-62489820
Fax: +86-21-62489821

IntechOpen